Journal of Inorganic Biochemistry 173 (2017) 134–140

Contents lists available at ScienceDirect

Journal of Inorganic Biochemistry

journal homepage: www.elsevier.com/locate/jinorgbio

Bis(diphenylphosphino)amines-containing ruthenium cymene complexes as potential anti-*Mycobacterium tuberculosis* agents

Juliana P. da Silva[a], Isabel C. Silva[b], Fernando R. Pavan[b], Davi F. Back[c], Márcio P. de Araujo[a,*]

[a] Departamento de Química, Universidade Federal do Paraná, Centro Politécnico, CP 19081, CEP 81531-980 Curitiba, PR, Brazil
[b] Departamento de Ciências Biológicas, Faculdade de Ciências Farmacêuticas, Univ. Estadual Paulista, CEP: 14800-900 Araraquara, SP, Brazil
[c] Departamento de Química, Universidade Federal de Santa Maria, CEP 97105-900 Santa Maria, RS, Brazil

ABSTRACT

Several ruthenium complexes have been investigated regarding anti-*Mycobacterium tuberculosis* (anti-MTb) activity, with some diphosphine-containing ruthenium complexes comparable to first and second line drugs. However, to the best of our knowledge, there is no P—N—P-containing ruthenium complexes applied as metallodrugs. Thus, this study focused on the synthesis, characterization and anti-MTb activity of a new series of coordination compounds with general formula [RuCl(η^6-*p*-cymene)(P—N^R—P)]X (R = CH_2Py (Py = pyridine) – **[1a]**, CH_2Ph (Ph = phenyl) – **[1b]**, Ph – **[1c]** and *p*-tol (*p*-tol = *p*-tolyl) – **[1d]**; X = PF_6^- or BF_4^-). The complexes were fully characterized by NMR (^{1}H, ^{31}P{^{1}H}), vibrational spectroscopy (FTIR), ESI-MS, molar conductance, elemental analysis and X-ray diffraction studies. The molecular structures of **[1a]·PF_6**, **[1c]·BF_4** and **[1d]·PF_6** were determined and confirm the spectroscopic and ESI-MS data. The complexes were used in anti-MTb trials, and the preliminary results are presented. The complexes are promising anti-MTb agents with MIC_{90} (Minimum Inhibitory Concentration of compounds required to inhibit the growth of 90% of MTb) values comparable with the Ethambutol, the reference drug used in this work, and complex **[1a]·BF_4** presented the highest selectivity index.

1. Introduction

There is broad consensus that the advancement of modern coordination chemistry is intimately linked to the development of the chemistry of tertiary phosphines, especially for coordination compounds involving the transition metals Ru, Rh and Ir [1–5]. The coordination chemistry of tertiary phosphines have been extensively explored due to their ability to stabilize the metal center in different oxidation states [1,6] and control the coordination environment around the metal center, consequence of steric hindrance and structural *trans* influence properties [7–9]. Among the tertiary phosphines, tertiary bis(diphenylphosphines) containing carbon backbone linking the two phosphorus donor atoms are of great impact in coordination chemistry and catalysis [10–13].

Another type of tertiary bis(diphenylphosphine) donor ligands is the bis(diphenylphosphino)amines, which contain a single nitrogen atom bridging the two phosphorus atoms, forming a P—N—P skeleton (Chart 1) [6,14].

The P—N—P ligands form a four-membered chelate ring size when coordinating to a metal center. The presence of a nitrogen atom bridging the two phosphorus atoms changes the properties of such ligands when compared with the more traditional diphosphines ($Ph_2P(CH_2)_nPPh_2$). For example, the $PPh_2(CH_2)PPh_2$ (bis[diphenylphosphino]methane – dppm) and PPh_2NHPPh_2 (bis[diphenylphosphino]amine – dppa) are isoelectronic, but their ^{31}P NMR chemical shift are − 23.6 [15] and 42.1 ppm [14], respectively. It is clear they have different electronic properties due to the lower electronegativity of the carbon compared to the nitrogen and the presence of a lone electron pair centered on nitrogen, which is delocalized over the P—N—P bonds through pz(N)-σ*(P—C) overlap [16] – as a result, the nitrogen atom is sp^2 hybridized.

One great advantage of the bis(diphenylphosphino) amines ligands compared to the traditional tertiary phosphines is the easy preparation and the availability of several commercial amines with different properties [17]. The ease of synthesis and the possibility to modulate the substituents on N and P positions can provide a wide range of ligands with different structural and electronic properties and makes the P—N—P ligands even more attractive for chemical applications [6,14].

In the past 10 years a large number of coordination compounds with this class of ligands have been explored, mainly in catalytic reactions

* Corresponding author.
E-mail address: mparaujo@ufpr.br (M.P. de Araujo).

http://dx.doi.org/10.1016/j.jinorgbio.2017.04.008
Received 27 November 2016; Received in revised form 6 April 2017; Accepted 8 April 2017
Available online 09 April 2017

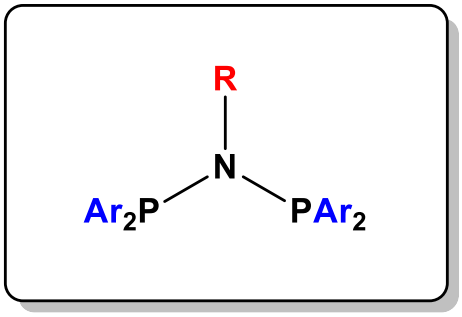

Chart 1. General representation of bis(diphenylphosphino)amine ligands.

including Heck [18], Suzuki [19], and hydrogenation [20]. Noteworthy is the importance of such compounds in industrial applications being used as ligand in chromium complexes for the production of 1-hexene and 1-octene from ethylene [21–24].

The majority of P—N—P-containing ruthenium compounds reported in the literature has an arene, such as *p*-cymene, benzene or cyclopentadienyl in their structures and is applied in catalytic transfer hydrogenation reactions [25–27]. However, it is known that Ru-arene is a promising class of compounds in the biological field with large number of anticancer active examples in the literature [28–32]. Furthermore, one of the most known and promising in this class, RAPTA-C, ruthenium–arene complex containing the phosphine 1,3,5-Triaza-7-phosphaadamantane (PTA), is currently on phase I clinical trial for cancer treatment [33]. Additionally, other phosphine-containing ruthenium complexes are also active against cancer cells, bacteria and *Mycobacterium tuberculosis* (MTb) [34–40].

Tuberculosis (TB) is mainly caused by MTb, and is one of the most threatening infectious diseases. According to the World Health Organization (WHO), in 2015 there were approximately 10.4 million new cases of tuberculosis in the world, and 1.4 million deaths attributed to TB (considering only HIV-negative people) [41]. Of those 5.6% are multi-drug resistant TB (MDR-TB), defined by the resistance to isoniazid and rifampicin.

In the past few years several ruthenium complexes have been investigated regarding anti-MTb activity, including one containing isoniazid as ligand [38,40,42,43]. Some diphosphine-containing ruthenium complexes, such as *cis*-[Ru(pic)(dppe)$_2$]PF$_6$ (pic = 2-picolinic acid; dppe = 1,2-bis(diphenylphosphino)ethane), presented MIC$_{90}$ comparable to first and second line drugs [40].

However, to the best of our knowledge, there is no P—N—P-containing ruthenium complexes applied as metallodrugs. Thus, this study focused on the synthesis, characterization and anti-MTb activity of a new series of coordination compounds with general formula [RuCl(η^6-p-cymene)(P–N^R–P)]X (Py = pyridine – **[1a]**, CH_2Ph (Ph = phenyl) – **[1b]**, Ph – **[1c]** and *p*-tol (*p*-tol = *p*-tolyl) – **[1d]**; X = PF_6^- or BF_4^-). Their use as anti-MTb agents can provides a new scaffold for the development of new metallodrugs.

2. Experimental section

2.1. Materials and instrumentation

Johnson Matthey plc donated commercially available $RuCl_3 \cdot 3H_2O$, and it was used as received. The $NaBF_4$ (Sigma-Aldrich) and KPF_6 (Sigma-Aldrich) salts were used without prior purification. The solvents were dried before use. All the manipulations involving solutions of the complexes were performed under argon atmosphere. [RuCl$_2$(η^6-*p*-cymene)]$_2$ and the P—N—P ligands were synthesized following the procedure published elsewhere [44–46].

NMR experiments were carried out at room temperature on a Bruker AVANCE 300 MHz. The ^{1}H and ^{31}P{^{1}H} NMR chemical shifts are given in ppm, relative to tetramethylsilane (TMS) and H_3PO_4 85% at 0 ppm, respectively. The coupling constants are given in Hz. ESI-MS were conducted on a Thermo Fisher Scientific Inc. LTQ XL Linear Ion Trap Mass Spectrometer with Software Xcalibur 2.1 processing, the sample concentrations in MeOH being ~10 μg mL^{-1}. Microanalysis was performed on a FISONS CHNS-O, mod. EA 1108 Element analyzer. Electrical conductivity measurements of solutions (1 mmol L^{-1}) of the complexes were performed on a DIGIMED DM-31 conductivimeter, at room temperature.

2.2. Preparations of the complexes [RuCl(η^6-p-cymene)(P—N^R—P)]X (R = CH_2Py – [1a], CH_2Ph – [1b], Ph – [1c] and p-tol – [1d]; X = PF_6^- or BF_4^-)

General procedure:

The P—N—P (197 μmol) ligand was added to a solution of [RuCl$_2$(η^6-*p*-cymene)]$_2$ (98.6 μmol) in MeOH (10 mL) and the resulting orange-yellow suspension was stirred under inert atmosphere, at room temperature, for a period of 3 h. After this time, the solution became yellow and the salt (NH_4PF_6 or $NaBF_4$ – 493 μmol) was added, with the resulting solution stirred for 30 min.

Among complexes containing PF_6^- as counter-ion, the product precipitated from the solution. The resulting yellow solid was filtered off, washed with water (5 mL), methanol (5 mL) and diethyl ether (5 mL), and dried under reduced pressure and heating (~80 °C) for 24 h.

The complexes containing BF_4^- needed one additional step to isolate the solid, due to the solubility of the compounds. The MeOH solution was concentrated under reduced pressure to 1 mL and diethyl ether was added to force the precipitation.

2.2.1. [RuCl(η^6-p-cymene)(P–N$_2^{CHpy}$—P)]BF$_4$ [1a]·BF$_4$

Yield: 90% (147 mg; 0.177 mmol). Elemental analysis calcd for $C_{40}H_{40}BClF_4N_2P_2Ru$: C 57.60; H 4.83; N 3.36. Found: C 57.78; H 4.89; N 3.14.^{1}H NMR ($CDCl_3$, 300 MHz): 8.05 (bd, (α - py)) 7.81–7.37 (m, $(PPh_2)_2$) 7.13 (td, *J* = 7.96 Hz, *J* = 1.54 Hz, 1H, py) 6.86 (dd, *J* = 7.78 Hz, *J* = 4.98 Hz, 1H, py) 6.06 (d, *J* = 6.04 Hz, 2H, Ar of *p*-cymene)), 5.97(d, *J* = 7.78 Hz, 1H, py), 5.81 (d, *J* = 6.04 Hz, 2H, Ar of *p*-cymene), 4.32 (t, *J* = 12,6 Hz, 2H, py-CH_2-N), 2.54 (spt, *J* = 7,13 1H, CH of *p*-cymene) 1.73 (bs, 3H, CH_3 of *p*-cymene), 1.10 (s, 6H, CH $(CH3)_2$ of *p*-cymene). ^{31}P {^{1}H} NMR ($CDCl_3$, 121.67 MHz): 80.34. ν/cm^{-1}: 1588 (C=C), 1437 (P—C_{Ar}), 1077 (B—F), 751 (P—N). ESI/MS (CH_2Cl_2) [M]$^+$ exp(calc): 747.22(747.14). Λ_m (CH_2Cl_2, μS·cm^2 mol^{-1}.): 35.48.

2.2.2. [RuCl(η^6-p-cymene)(P—N$_2^{CHPh}$—P)]BF$_4$ [1b]·BF$_4$

Yield: 94% (154 mg; 0.185 mmol). Elemental analysis calcd. for $C_{41}H_{41}BClF_4NP_2Ru$: C 59.11; H 4.96; N 1.68. Found: C 58.98; H 4.98; N 1.61. ^{1}H NMR ($CDCl_3$, 300 MHz): 7.73–7.34 (m, 20H $(PPh_2)_2$) 6.86–7.10 (m, 3H, Ar-CH_2Ph) 6.51 (bd, Aromatic (Ar) CH_2Ph) 6.07 (d, *J* = 6.30 Hz, 2H, Ar of *p*-cymene), 5.89(d, *J* = 6.30 Hz, 1H, Ar of *p*-cymene), 4.24 (t, *J* = 12,5 Hz, 2H, Ph-CH_2-N), 2.62 (spt, *J* = 7,02 1H, CH of *p*-cymene) 1.73 (bs, 3H, CH_3 of *p*-cymene), 1.10 (s, 6H, $CH(CH3)_2$ of *p*-cymene). ^{31}P {^{1}H} NMR ($CDCl_3$, 121.67 MHz): 80.65. ν/cm^{-1}: 1588 (C=C), 1437 (P—C_{Ar}), 1077 (B—F), 752 (P—N). ESI/MS (CH_2Cl_2) [M]$^+$ exp(calc): 746.12(746.14). Λ_m (CH_2Cl_2, μS·cm^2 mol^{-1}.): 49.53.

2.2.3. [RuCl(η^6-p-cymene)(P—N^{Ph}—P)]BF$_4$ [1c]·BF$_4$

Yield: 89% (143 mg, 0.175 mmol). Elemental analysis calcd. for $C_{40}H_{39}BClF_4NP_2Ru$: C 58.66; H 4.80; N 1.71. Found: C 58.70; H 4.87; N, 1.54. ^{1}H NMR ($CDCl_3$, 300 MHz): 7.75–7.34 (m, 20H $(PPh_2)_2$), 7.12–6.95 (m, 3H, Ar - aniline) 6.59 (bd, 2H, Ar-aniline), 6.11 (d, *J* = 6.30 Hz, 2H, Ar of *p*-cymene), 5.88 (d, *J* = 6.30 Hz, 2H, Ar of *p*-cymene), 2.57 (spt, *J* = 7.03 Hz, 1H, CH of *p*-cymene), 1.72 (bs, 3H, CH_3 of *p*-cymene), 1.14 (s, 6H, $CH(CH_3)_2$ of *p*-cymene). ^{31}P {^{1}H} NMR

($CDCl_3$, 121.67 MHz): 79.46. ν/cm^{-1}: 1588 (C═C), 1437 (P−C_{Ar}), 1232 (N−C_{Ar}), 1077 (B−F), 752 (P−N). ESI/MS (CH_2Cl_2) $[M]^+$ exp (calc): 732.15(732.13). Λ_m (CH_2Cl_2, μS·cm^2 mol^{-1}.): 36.69.

2.2.4. [RuCl(η^6-p-cymene)(P−$N^{p\text{-}tol}$−P)]BF_4 [1d]·BF_4

Yield: 82% (134 mg; 0.161 mmol). Elemental analysis calcd. for $C_{41}H_{41}BClF_4NP_2Ru$: C 59.11; H 4.96; N 1.68. Found: C 58.88; H 4.95; N, 1.46. ^{1}H NMR ($CDCl_3$, 300 MHz): 7.65–7.30(m, 20H $(PPh_2)_2$), (d, J = 8.30 Hz, 2H, Ar-*p*-tol) 6.45 (d, J = 8.30 Hz, 2H, Ar-*p*-tol) 6.03 (d, J = 6.02 Hz, 2H, Ar of *p*-cymene), 5.76 (d, J = 6.02 Hz, 2H, Ar of *p*-cymene), 2.53 (spt, J = 6,95 1H, CH of *p*-cymene), 2.17 (bs, 3H, CH_3 of *p*-cymene) 1.66 (bs, 3H, CH_3 – *p*-tol), 1.11 (s, 6H, $CH(CH_3)_2$ of *p*-cymene). ^{31}P {^{1}H} NMR ($CDCl_3$, 121.67 MHz): 78.80. ν/cm^{-1}: 1588 (C═C), 1435 (P−C_{Ar}), 1232 (N−C_{Ar}), 1081 (B−F), 753 (P−N) ESI/MS (CH_2Cl_2) $[M]^+$ exp(calc): 746.15(746.14). Λ_m (CH_2Cl_2, μS·cm^2-mol^{-1}.): 44.82.

*The spectroscopic data for complexes **[1a] – [1d] PF_6** are virtually the same of the BF_4^- analogues, except for the ^{31}P NMR spectra, in which the PF_6^- signal was observed at − 142 ppm.

2.3. X-ray diffraction data

X-ray quality single-crystals of **[1a] ·PF_6**, **[1c] ·BF4** and **[1d] ·BF_4** were grown by layering CH_2Cl_2 solutions of the complexes with diethyl ether. Crystal data and structure refinement are summarized in Table 1. The molecular structures were solved on a Bruker APEX II CCD diffractometer, at 293 K, using graphite-monochromatized Mo Kα radiation (0.71073 Å). The structures were solved by direct method using SHELXS [47]. Subsequent Fourier-difference map analyses provided the positions of the non-H-atoms with refinements carried out with the SHELXL package using full–matrix least squares on F^2 with anisotropic displacement parameters [48]. H-atoms were included in the refinement at the calculated positions.

2.3.1. Anti-Mycobacterium tuberculosis activity

The antitubercular activity of the compounds was determined through the REMA methodology as described by Palomino et al. [49]. Stock solutions of the tested compounds were prepared in DMSO (Sigma-Aldrich®) and diluted in Middlebrook 7H9 broth (Difco) supplemented with 10% OADC enrichment (dextrose, albumin, and catalase — BBL/Becton-Dickinson), to obtain final drug concentration ranges of 0.09–25 μg mL^{-1}. Ethambutol (Sigma-Aldrich®) was used as a standard drug. A suspension of the MTB H_{37}Rv ATCC 27294 was cultured in Middlebrook 7H9 broth supplemented with 10% OADC and 0.05% Tween 80. The concentration was adjusted to 2×10^5 UFC mL^{-1} and 100 μL of the inoculum was added to each well of a 96-well microtiter plate together with 100 μL of the compounds. Samples were set up in triplicate. The plate was incubated for 7 days at 37 °C. After 24 h 30 μL of 0.01% resazurin (solubilized in distilled water) was added. The fluorescence of the wells was read in a Cytation 3 (Biotek®) in which excitations and emissions filters were used at wavelengths of 530 and 590 nm, respectively. Each test was set up in triplicate.

2.3.2. Cell culture

MRC-5 cells (human lung fibroblast cell line) were obtained from the American Type Culture Collection (Manassas, VA, USA) and incubated in DMEM medium and supplemented with 10% FBS and 1% penicillin (100 U/mL)–streptomycin (100 μg mL^{-1}). Cells were maintained in a humidified environment at 37 °C with 5% CO_2 and sub-cultured twice per week.

2.3.3. Cytotoxicity tests

The cytotoxicity was measured fluorometrically by the resazurin reduction assay. Resazurin is a non-toxic and non-fluorescent blue reagent that is reduced to fluorescent and pink-colored resorufin by viable cells. Nonviable cells rapidly lose the metabolic capacity to reduce resazurin and thus do not produce a fluorescent signal.

Briefly, 2.5×10^4 cells/well were seeded in a 96-well cell culture plate (Costar, USA) in a total volume of 100 μl for 24 h, and then treated with concentrations of substances ranging from 200 to 1.6 μg L^{-1}. After 24 h incubation, the medium was removed and 50 μL resazurin (Sigma–Aldrich, Germany) 0.01% w/v in DMEM, was added to each well and the plates were incubated at 37 °C for 3 h.

Table 1
Crystal data and structure refinement for **[1a] ·PF_6**, **[1c] ·BF4** and **[1d] ·PF_6**.

Data	[1a]·PF_6	[1c]·BF4	[1d]·PF_6
Empirical formula	$C_{40}H_{40}ClF_6N_2P_3Ru$	$C_{40}H_{39}BClF_4NP_2Ru$	$C_{41}H_{41}ClF_6NP_3Ru$
Formula weight	892.17	818.99	891.18
Temperature	293(2) K	293(2) K	290(2) K
Wavelength	0.71073 Å	0.71073 Å	0.71073 Å
Crystal system, space group	Triclinic, *P*-1	Monoclinic, *P*21/*c*	Orthorhombic, *P*212121
Unit cell dimensions	a = 10.6394 (3) Å α = 84.287 (1)° b = 12.3708 (3) Å β = 89.016 (1)° c = 15.6032 (4) Å γ = 81.740 (1)°	a = 18.2802 (4) Å α = 90° b = 11.4332 (2) Å β = 102.6390 (10)° c = 18.7011 (4) Å γ = 90°	a = 11.6128(3) (4) Å α = β = γ = 90° b = 18.1369(4) Å c = 18.9502(5) Å
Volume	2022.25 (9) A^3	3813.84 (9) A^3	3991.30(17) A^3
Z, Density (calculated)	2, 1.465 Mg/m^3	4, 1.426 Mg/m^3	4, 1.483 Mg/m^3
Absorption coefficient	0.631 mm^{-1}	0.614 mm^{-1}	0.639 mm^{-1}
F(000)	908	1672	1816
Crystal size	0.766 × 0.525 × 0.504 mm	0.275 × 0.206 × 0.129 mm	0.426 × 0.226 × 0.112 mm
Theta range for data collection	1.31–27.18°	1.14–27.18°	2.06–27.63°
Index ranges	− 13 ≤ h ≤ 13, − 15 ≤ k ≤ 15, − 20 ≤ l ≤ 19	− 23 ≤ h ≤ 23, − 14 ≤ k ≤ 14, − 24 ≤ l ≤ 23	− 15 ≤ h ≤ 15, − 23 ≤ k ≤ 23, − 24 ≤ l ≤ 24
Reflections collected	55,560	56,119	58,660
Independent reflections	8965 [R(int) = 0.0183]	8445 [R(int) = 0.0716]	9273 [R(int) = 0.0411]
Completeness to θ	99.6% (27.19°)	99.7% (27.18°)	99.8% (27.63°)
Absorption correction	Gaussian	Gaussian	Numerical
Max. and min. Transmission	0.8686 and 0.7927	0.9267 and 0.8636	0.7456 e 0.6973
Refinement method	Full-matrix least-squares on F^2	Full-matrix least-squares on F^2	Full-matrix least-squares on F^2
Final R indices [I > 2sigma (I)]	R1 = 0.0318, w$R2$ = 0.0877	R1 = 0.0429, w$R2$ = 0.0912	R1 = 0.0293, w$R2$ = 0.0652
R indices (all data)	R1 = 0.0352, w$R2$ = 0.0918	R1 = 0.0816, w$R2$ = 0.1061	R1 = 0.0365, w$R2$ = 0.0686
Largest diff. peak and hole	0.947 e − 0.690 e·A^{-3}	0.671 e − 0.545 e·A^{-3}	0.351 e − 0.278 e·A^{-3}

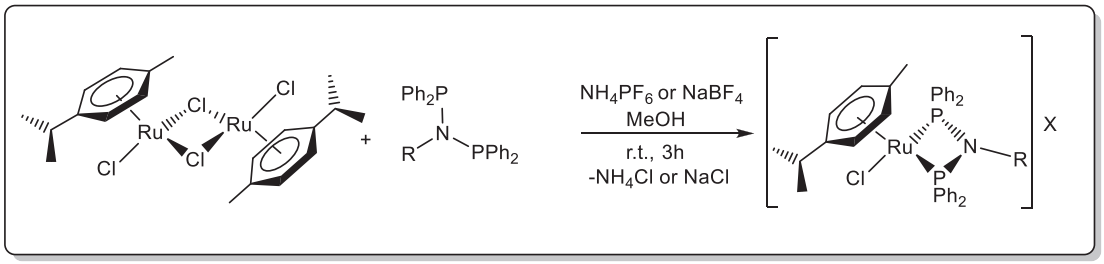

Scheme 1. Preparation of complexes **[1a]–[1d]·X** (X = BF_4^- or PF_6^-). R = CH_2py **[1a]**, CH_2Ph **[1b]**, Ph **[1c]**, and *p*-tol **[1d]**.

The fluorescence was measured on Biotek Synergy H1 plate reader (Biotek, Winooski, VT) using an excitation wavelength of 530 nm and an emission wavelength of 590 nm. Untreated cells constituted the negative control (viable cells), cell treated with DMSO 1% and doxorubicin at 100 nmol (Sigma-Aldrich, St. Louis, MO, USA) constituted the vehicle and positive controls (dead cells), respectively. All the tests were performed in three independent assays.

The IC_{50} values represent the concentrations of the samples required to inhibit 50% of cell proliferation and were calculated from a calibration curve by regression curves.

3. Results and discussion

3.1. Synthesis and characterization of complexes [1a]–[1d]·X (X = BF_4^- or PF_6^-)

The complexes were synthesized following the route presented in Scheme 1. All complexes were isolated as yellow or orange-yellow solid and were characterized by $^{31}P\{^1H\}$, ^1H NMR, ESI-MS, elemental analysis, molar conductance and the solid state molecular structures of complexes **[1a]·PF_6**, **[1c]·BF4** and **[1d]·PF_6** were determined by X-ray crystallography, and the NMR data in solution are consistent with the structures stablished by X-ray crystallography.

The molar conductance values of all complexes are in the range 35.48–49.53 $\mu S \cdot cm^2\ mol^{-1}$ (1 mmol L^{-1} CH_2Cl_2 solution), which are in the accepted range for 1:1 electrolytes [35].

3.2. X-ray diffraction structures for complexes [1a]·PF_6, [1c]·BF_4 and [1d]·PF_6.

Single crystals were obtained by slow evaporation of a dichloromethane solution of complexes **[1a]·PF_6**, **[1c]·BF_4** and **[1d]·PF_6**. Molecular structures of these complexes are shown in Figs. 1–3,

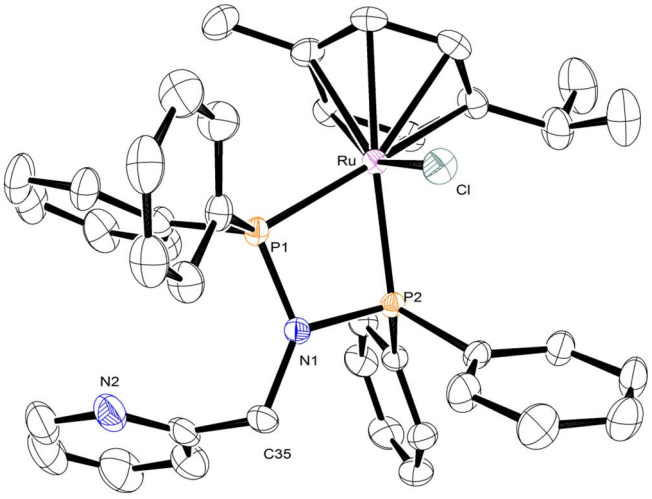

Fig. 1. Representation of the **[1a]·PF_6** structure, with 30% probability thermal ellipsoids; H-atoms and PF_6^- are omitted for clarity.

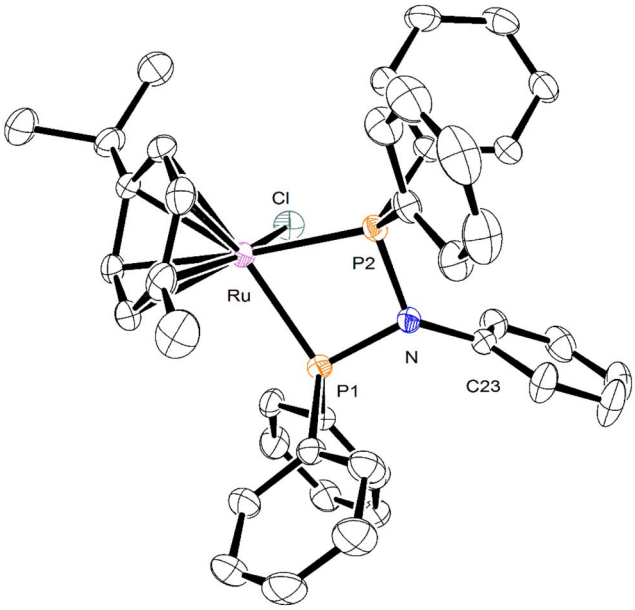

Fig. 2. Representation of the **[1c]·BF_4** structure, with 30% probability thermal ellipsoids; H-atoms and BF_4^- are omitted for clarity.

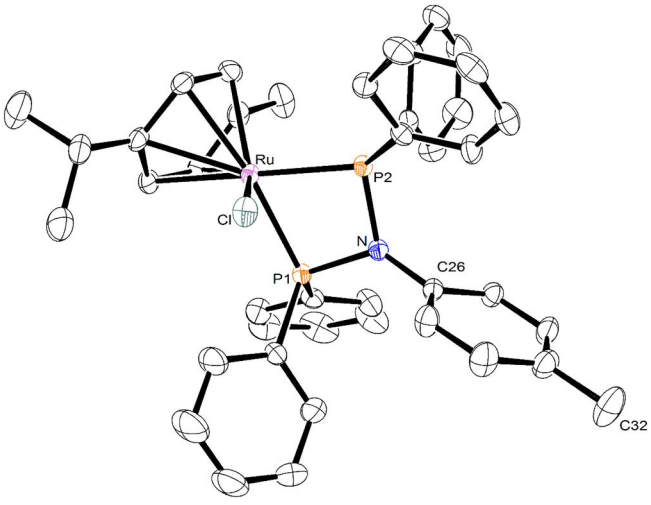

Fig. 3. Representation of the **[1d]·PF_6** structure, with 30% probability thermal ellipsoids; H-atoms and PF_6^- are omitted for clarity.

respectively, and the relevant bond lengths and angles are summarized in Table 2.

All complexes presented the typical three legged piano-stool (distorted) geometry, in which the Ru (II) center is coordinated by *p*-cymene, chelated P—N—P ligand and one chlorido.

The Ru—C bond lengths (2.190(3)–2.328(3) Å) are in a range comparable to the bond lengths found for the analogues complexes [RuCl(η^6-*p*-cymene)(P—P)]BF_4 (P—P = bis[diphenylphosphino]methane

Table 2
Selected metric parameters for [1a]·PF_6, [1c]·BF_4 and [1d]·PF_6.

	[1a]·PF_6		[1c]·BF_4		[1d]·PF_6	
Bond lengths (Å)	Ru—P1	2.3043(8)	Ru—P1	2.2884(9)	Ru—P1	2.3077(6)
	Ru—P2	2.3020(8)	Ru—P2	2.3010(9)	Ru—P2	2.2948(6)
	Ru—Cl	2.3813(8)	Ru—Cl	2.3933(9)	Ru—Cl	2.3763(7)
	P1—N1	1.692(3)	P1—N	1.710(3)	P1—N	1.711(2)
	P2—N1	1.697(3)	P2—N	1.703(3)	P2—N	1.7102(19)
	Ru—C(4)	2.2079(2)	Ru—C1	2.309(3)	Ru—C(37)	2.190(3)
	Ru—C(3)	2.2343(2)	Ru—C2	2.255(4)	Ru—C(36)	2.244(3)
	Ru—C(7)	2.2610(2)	Ru—C3	2.223(4)	Ru—C(35)	2.243(3)
	Ru—C(6)	2.2635(2)	Ru—C4	2.243(4)	Ru—C(34)	2.263(2)
	Ru—C(5)	2.284(3)	Ru—C5	2.195(4)	Ru—C(38)	2.282(3)
	Ru—C(2)	2.289(3)	Ru—C6	2.273(4)	Ru—C(33)	2.328(3)
Bond angles (°)	P2—Ru—P1	68.81(3)	P1—Ru—P2	69.03(3)	P1—Ru—P2	69.18(2)
	P1—Ru—Cl	87.68(3)	P1—Ru—Cl	85.57(3)	P1—Ru—Cl	84.35(3)
	P2—Ru—Cl	86.26(3)	P2—Ru—Cl	82.90(3)	P2—Ru—Cl	82.93(3)
	P1—N1—P2	100.32(14)	P1—N—P2	99.27(14)	P1—N—P2	99.60(11)
	C35—N1—P1	133.9(2)	C23—N—P1	126.8(2)	C23—N—P1	129.71(16)
	C35—N1—P2	125.7(2)	C23—N—P2	130.2(2)	C23—N—P2	129.18(17)

– dppm or dppe) [50]. On the other hand, the Ru—P bond lengths for the complexes **[1a]·PF_6**, **[1c]·BF_4** and **[1d] vPF_6** (2.2884(9)–2.3077(6) Å) are smaller than the range observed for [RuCl(η⁶-*p*-cymene)(P—P)]BF_4 (P-P = dppm or dppe) (2.309(2)–2.336(1) Å), and the Ru—Cl bond lengths (2.3763(7)–2.3933(9) Å) are also smaller than the values observed for [RuCl(η⁶-*p*-cymene)(dppm)]BF_4 and [RuCl(η⁶-*p*-cymene)(dppe)]BF_4, 2.397(2) and 2.430 (1) Å, respectively [50]. The shorter Ru—P and Ru—Cl bond lengths for complexes **[1a·PF_6**, **[1c]·BF_4** and **[1d]·PF_6** compared with their analogues with dppm and dppe may be due to the possible lesser donor (and stronger π-acceptor) strength of the P—N—P ligands of this work.

The P—Ru—P bond angles for **[1a]·PF_6** – 68.81(3)°, **[1c]·BF_4** – 69.03(3)° and **[1d]·PF_6** – 69.18(2)° are smaller than those observed for the analogue with dppm,71.29(6)° [50]. Worth noting is the compression in the P—N—P versus P—C—P bond angles of the free ligand compared to the coordinated one. For example, the P—N—P bond angle for free P—N^{Mepy}—P is 121.8(1)° [16] and coordinated is 100.32(14)° (complex **[1a]·PF6**), while for dppm, the bond angle for the free ligand is 107.63(10)° and upon coordination the angle in compressed to 95.3(3)° [50]. The strong compression observed for the P—N—P ligands may be a consequence of the bulky R substituents on nitrogen atoms.

3.3. NMR data

The $^{31}P\{^1H\}$ NMR spectra show one singlet in the region 78.80–80.65 ppm, compatible with the chelated P—P coordination fashion.

The ^1H NMR data (assignments and integrations) are straightforward; the main features of the ^1H NMR spectra are as follows: The aromatic hydrogen atoms of *p*-cymene are observed as two doublets in the region 6.11–5.76 ppm ($^3J \sim 6$ Hz). The aromatic hydrogen atoms of –P*Ph*$_2$ are observed in the region 7.81–7.30 ppm. Additionally, the complex **[1a]·BF_4** presents one broad doublet at 8.05 ppm characteristic of the o-H-py; the complexes **[1a]·BF_4** and **[1b]·BF_4** present one triplet at 4.32 and 4.24 ppm, respectively, attributed to the C*H*$_2$ with $^3J_{H\text{-}P} \sim 12$ Hz; and the complex **[1d]·BF_4** one broad singlet at 1.66 ppm due to the presence of *p*-CH_3.

3.4. ESI-MS data

The gas-phase behavior of **[1a]–[1d]·BF_4** was achieved by ESI-MS using CH_2Cl_2 solutions of the complexes. The full-scan mode generated the molecular ion, [M^+] for each complex, which is in agreement with the calculated *m/z* ratio and isotopic pattern. The same fragmentation pathway of the [M]$^+$ is observed for all complexes, generating the ions [M – cymene]$^+$, [M − Cl]$^+$ and [M − cymene − Cl]$^+$.

3.5. Anti-Mycobacterium tuberculosis activity

The complexes **[1a]–[1d]·X** (X = PF_6^- or BF_4^-), precursor [$RuCl_2$(η⁶-*p*-cymene)]$_2$ and the P—N—P ligands were evaluated as anti-MTb agents and the MIC_{90} values were determined. In addition, the cytotoxicity (IC_{50}) and the selectivity index (SI) were also determined for the complexes **[1a]–[1d]·X** (X = PF_6^- or BF_4^-), and all the results are summarized in Table 3. The MIC_{90} and IC_{50} were determined using stock solutions of the complexes in DMSO, medium in which the complexes are stable for at least 7 days, as evidenced by 31P {1H} NMR.

Table 3
Anti-*Mycobacterium tuberculosis* activity (MIC_{90}), cytotoxicity (IC_{50}), and selectivity index (SI) for **[1a]·X** and **[1b]·X** (X = PF_6^- or BF_4^-).

Complexes	MIC_{90} (μg mL^{-1})[a]	MIC_{90} (μmol L^{-1})	IC_{50} (μg mL^{-1})	IC_{50} (μmol L^{-1})	SI[b]
[$RuCl_2$(η⁶–*p*–cymene)]$_2$	> 25	> 41	–	–	–
P–N^{CH2Py}–P	> 25	> 52	–	–	–
P–N^{CH2Ph}–P	> 25	> 53	–	–	–
P–N^{Ph}–P	> 25	> 54	–	–	–
P–$N^{p\text{-}tol}$–P	> 25	> 53	–	–	–
[RuCl(η⁶–*p*–cymene)(P–N_2^{CHpy}–P)] PF_6 [1a]·PF_6	12.5 ± 0.9	14.0 ± 1.0	38	42	3.0
[RuCl(η⁶–*p*–cymene)(P–N_2^{CHPh}–P)] PF_6 [1b]·PF_6	3.6 ± 0.3	4.0 ± 0.3	5.0	5.6	1.4
[RuCl(η⁶–*p*–cymene)(P–N_2^{CHpy}–P)]BF_4 [1a]·BF_4	3.6 ± 0.8	4.3 ± 0.9	58	69	16
[RuCl(η⁶–*p*–cymene)(P–N_2^{CHPh}–P)]BF_4 [1b]·BF_4	3.6 ± 0.5	4.3 ± 0.6	7.0	8.4	2.0

All complexes, including the precursor, were tested in DMSO and the ligands in CH_2Cl_2 solutions.
Ethambutol MIC_{90} = 5.62 μmol L^{-1}.
[a] The complexes **[1c]·X** and **[1d]·X** (X = PF_6^- or BF_4^-) presented MIC > 25 μg mL^{-1}.
[b] SI = IC_{50}/MIC_{90}.

The complexes **[1a]·X** and **[1b]·X** (X = PF_6^- or BF_4^-) have shown promising results, with $MIC_{90} \leq 12.5\ \mu g\ mL^{-1}$ (14.0 μmol L^{-1}), while the complexes **[1c]·X** and **[1d]·X** (X = PF_6^- or BF_4^-) are not active in the concentration range tested ($MIC_{90} > 25\ \mu g\ mL^{-1}$). The same lack of activity was also observed for the $[RuCl_2(\eta^6\text{-}p\text{-cymene})]_2$ and the free P—N—P ligands. The complex **[1a]·PF_6** is the less active, and the complexes **[1b]·PF_6**, **[1a]·BF_4** and **[1b]·PF_6** have essentially the same MIC_{90} values. These MICs are lower than the value for the reference drug Ethambutol (see caption of Table 3).

The cytotoxicity of the complexes **[1a]–[1d]·X** (X = PF_6^- or BF_4^-) (Table 3) against healthy cells(MCR-5 cell) are in the range 5.6–69 μmol L^{-1}. The selectivity index (SI) found is in the range 1.4–16. According to Orme et al. [51], complex **[1a]·BF_4**, (SI = 16 and $MIC_{90} = 3.6\ \mu g\ mL^{-1}$) is the most promising as anti-MTB metallodrug, since this complex has SI ≥ 10 and MIC90 < $6.25\ \mu g\ mL^{-1}$.

It seems that the basicity of the amines, which can affect the donor ability of the P—N—P ligands, may be related to the activity of the complexes. The phosphines $P—N^{Ph}—P$ and $P—N^{p\text{-tol}}—P$ are derived from the least basic amines, aniline (pKa = 4.6) [52] and p-tolylaniline (pKa = 5.2) [52], and their complexes are inactive in the concentration range studied. On the other hand, the phosphines $P—N^{CH2Py}—P$ and $P—N^{CH2Ph}—P$, derived from the most basic amine − 2-aminomethylpyridine (pKa = 8.8) [53] and 2-benzylamine (pKa = 9.3) [54], generated the most active complexes in this work. Additionally, the presence of non-bonded pyridyl in **[1a]** may also play a role, for example in interaction with the mycolic acids present in the membrane of MTb.

Turning to the counter-ion effect (PF_6^- vs BF_4^-) for the anti-MTb assays, it was observed that **[1a]·BF_4** is 3.5 times more active than the **[1a]·PF_6**. However, for the cytotoxic assays, the PF_6^--containing complexes are more toxic than the BF_4^--ones. On the other hand, the cytotoxicity is markedly affected by the nature of the cation, **[1a]** is at least 7.5 times less toxic than **[1b]**.

The anti-MTb activities of the complexes assayed in this work are lower than other ruthenium–diphosphines complexes published elsewhere. Batista and co-workers, including the third author of this paper, have reported the anti-MTb activity of several ruthenium complexes; for example, the complexes $[Ru(SpymMe_2)(dppb)(bipy)]PF_6$ (SpymMe$_2$ = 4,6-dimethyl-2-mercaptopyrimidine; dppb = 1,4-bis[diphenylphosphino]butane; bipy = 2,2′-bipyridine) and *cis*-$[Ru(pic)(dppe)_2]PF_6$ presented MIC_{90} 0.80 and 0.22 μmol L^{-1} [39,40].

4. Conclusions

Complexes with general formula $[RuCl(\eta^6\text{-p-cymene})(P—N^R—P)]X$ (R = CH_2Py − **[1a]**, CH_2Ph − **[1b]**, Ph − **[1c]** and *p*-tol − **[1d]**; X = PF_6^- or BF_4^-) were successfully synthesized. The X-ray analysis revealed the typical piano-stool structure around the ruthenium center. As expected, the geometry around the bridging nitrogen atoms is trigonal planar and compatible with sp^2 hybridization. The complexes were assayed as anti-*Mycobacterium tuberculosis* and showing good activity. Complexes **[1c]·X** and **[1d]·X** were less active with $MIC_{90} > 25\ \mu g\ mL^{-1}$. On the other hand, the complexes **[1b]·PF_6**, **[1a]·BF_4** and **[1b]·BF_4** presented the same activity ($3.6\ \mu g\ mL^{-1}$), while **[1b]·PF_6** showed MIC90 $12.5\ \mu g\ mL^{-1}$. Of particular note is the fact that both metal precursor and free ligands are inactive, while the $P—N^R—P$ containing complexes (R=CH_2-py and CH_2—Ph) are highly active. The structure of P—N—P ligand has great influence on the activity of the complexes. The complexes containing the aniline derived P—N—P ligands are less active than the ones derived from 2-ampy and benzylamine, indicating that basicity may play a role. As stated earlier, the great advantage of P—N—P type ligands used in this work is the relative ease of synthesis and the modulation of the properties just by changing the amine type used in the reaction. In this way, P—N—P—containing complexes can be said to hold promise as a class of compounds to be applied as metallodrugs.

Acknowledgements

The authors are grateful to CNPq, CAPES (PROCAD/NF 2009 and CAPES/UdelaR 2010), FINEP and Fundação Araucária for financial support, to Johnson Matthey plc for the loan of $RuCl_3 \cdot xH_2O$ (to M.P.A.), and the Academic Publishing Advisory Center (*Centro de Assessoria de Publicação Acadêmica*, *CAPA* - www.capa.ufpr.br) of the Federal University of Paraná for assistance with English language editing. J.P.S. also thanks CNPQ for the SWE fellowship award.

Appendix A. Supplementary data

$^{31}P\{^1H\}$ and ^1H NMR, and ESI-MS spectra (pdf). Crystallographic information file for **[1a]·PF_6**, **[1c]·BF_4** and **[1d]·PF_6** (CIF).

Crystal data and structure refinement, $^{31}P\{^1H\}$ and ^1H NMR, and ESI-MS spectra (pdf). Crystallographic information file for **[1a]·PF_6**, **[1c]·BF_4** and **[1d]·PF_6** (CIF).

Crystallographic data for **[1a]·PF_6**, **[1c]·BF_4** and **[1d]·PF_6** have been deposited with the Cambridge Crystallographic Data Centre with CCDC numbers 1475474, 1475475 and 1475476, respectively. The data can be obtained free of charge, via www.ccdc.cam.ac.uk/conts/retrieving.html (or from the Cambridge Crystallographic Data Centre, CCDC, 12 Union Road, Cambridge CB2 1EZ, UK; fax: +44 1223 336,033; or e-mail: deposit@ccdc.cam.ac.uk). Supplementary data associated with this article can be found in the online version, at http://dx.doi.org/10.1016/j.jinorgbio.2017.04.008.

References

[1] T.A. Stephenson, G. Wilkinson, New complexes of ruthenium (II) and (III) with triphenylphosphine, triphenylarsine, trichlorostannate, pyridine and other ligands, J. Inorg. Nucl. Chem. 28 (1966) 945–956.
[2] D. Evans, J.A. Osborn, G. Wilkinson, Hydroformylation of alkenes by use of rhodium complex catalysts, J. Chem. Soc. A (1968) 3133–3142, http://dx.doi.org/10.1039/J19680003133.
[3] P.S. Hallman, T.A. Stephenson, G. Wilkinson, Tetrakis(triphenylphosphine)dichloro-ruthenium(II) and tris(triphenylphosphine)-dichlororuthenium(II), Inorg. Synth. 12 (1970).
[4] J.A. Osborn, F.H. Jardine, J.F. Young, G. Wilkinson, The preparation and properties of tris(triphenylphosphine)halogenorhodium(I) and some reactions thereof including catalytic homogeneous hydrogenation of olefins and acetylenes and their derivatives, J. Chem. Soc. A (1966) 1711–1732, http://dx.doi.org/10.1039/J19660001711.
[5] L. Vaska, R.E. Rhodes, Homogeneous catalytic hydrogenation of ethylene and acetylene with four-coordinated iridium and rhodium complexes. Reversible catalyst-substrate adducts1, J. Am. Chem. Soc. 87 (1965) 4970–4971.
[6] T. Appleby, J. Derek Woollins, Inorganic backbone phosphines, Coord. Chem. Rev. 235 (2002) 121–140.
[7] C.A. Tolman, Electron donor-acceptor properties of phosphorus ligands. Substituent additivity, J. Am. Chem. Soc. 92 (1970) 2953–2956.
[8] C.A. Tolman, Steric effects of phosphorus ligands in organometallic chemistry and homogeneous catalysis, Chem. Rev. 77 (1977) 313–348.
[9] B.J. Coe, S.J. Glenwright, Trans-effects in octahedral transition metal complexes, Coord. Chem. Rev. 203 (2000) 5–80.
[10] R. Noyori, H. Takaya, BINAP: an efficient chiral element for asymmetric catalysis, Acc. Chem. Res. 23 (1990) 345–350.
[11] K. Abdur-Rashid, M. Faatz, A.J. Lough, R.H. Morris, Catalytic cycle for the asymmetric hydrogenation of prochiral ketones to chiral alcohols: direct hydride and proton transfer from chiral catalysts trans-Ru(H)2(diphosphine)(diamine) to ketones and direct addition of dihydrogen to the resulting hydridoamido complexes, J. Am. Chem. Soc. 123 (2001) 7473–7474.
[12] G. Chelucci, S. Baldino, W. Baratta, Ruthenium and osmium complexes containing 2-(aminomethyl)pyridine (Ampy)-based ligands in catalysis, Coord. Chem. Rev. 300 (2015) 29–85.
[13] W.S. Knowles, M.J. Sabacky, B.D. Vineyard, D.J. Weinkauff, Asymmetric hydrogenation with a complex of rhodium and a chiral bisphosphine, J. Am. Chem. Soc. 97 (1975) 2567–2568.
[14] P. Bhattacharyya, J.D. Woollins, Bis(diphenylphosphino)amine and related chemistry, Polyhedron 14 (1995) 3367–3388.
[15] O. Kühl, Phosphorus-31 NMR Spectroscopy: A Concise Introduction for the Synthetic Organic and Organometallic Chemist, Springer, 2008.
[16] D. Olbert, A. Kalisch, N. Herzer, H. Görls, P. Mayer, L. Yu, M. Reiher, M. Westerhausen, Syntheses of *N*-(diphenylphosphanyl)-2-pyridylmethylamine and its use as a ligand in magnesium and zinc complexes, Z. Anorg. Allg. Chem. 633 (2007) 893–902.
[17] L.M. Broomfield, Y. Wu, E. Martin, A. Shafir, Phosphino-amine (PN) ligands for rapid catalyst discovery in ruthenium-catalyzed hydrogen-borrowing alkylation of

anilines: a proof of principle, Adv. Synth. Catal. 357 (2015) 3538–3548.
[18] C. Kayan, N. Biricik, M. Aydemir, Aminophosphine ligands: synthesis, coordination chemistry, and activity of their palladium(II) complexes in Heck and Suzuki cross-coupling reactions, Transit. Met. Chem. 36 (2011) 513–520.
[19] M. Aydemir, F. Durap, A. Baysal, O. Akba, B. Gümgüm, S. Özkar, L.T. Yıldırım, Synthesis and characterization of new bis(diphenylphosphino)aniline ligands and their complexes: X-ray crystal structure of palladium(II) and platinum(II) complexes, and application of palladium(II) complexes as pre-catalysts in Heck and Suzuki cross-coupling reactions, Polyhedron 28 (2009) 2313–2320.
[20] M. Aydemir, N. Meric, C. Kayan, F. Ok, A. Baysal, Rhodium-catalyzed transfer hydrogenation with functionalized bis(phosphino)amine ligands, Inorg. Chim. Acta 398 (2013) 1–10.
[21] A. Carter, S.A. Cohen, N.A. Cooley, A. Murphy, J. Scutt, D.F. Wass, High activity ethylene trimerisation catalysts based on diphosphine ligands, Chem. Commun. (2002) 858–859, http://dx.doi.org/10.1039/B201335E.
[22] A. Bollmann, K. Blann, J.T. Dixon, F.M. Hess, E. Killian, H. Maumela, D.S. McGuinness, D.H. Morgan, A. Neveling, S. Otto, M. Overett, A.M.Z. Slawin, P. Wasserscheid, S. Kuhlmann, Ethylene tetramerization: a new route to produce 1-octene in exceptionally high selectivities, J. Am. Chem. Soc. 126 (2004) 14712–14713.
[23] S. Kuhlmann, K. Blann, A. Bollmann, J.T. Dixon, E. Killian, M.C. Maumela, H. Maumela, D.H. Morgan, M. Pretorius, N. Taccardi, P. Wasserscheid, N-substituted diphosphinoamines: toward rational ligand design for the efficient tetramerization of ethylene, J. Catal. 245 (2007) 279–284.
[24] K. Blann, A. Bollmann, H. de Bod, J.T. Dixon, E. Killian, P. Nongodlwana, M.C. Maumela, H. Maumela, A.E. McConnell, D.H. Morgan, M.J. Overett, M. Pretorius, S. Kuhlmann, P. Wasserscheid, Ethylene tetramerisation: subtle effects exhibited by N-substituted diphosphinoamine ligands, J. Catal. 249 (2007) 244–249.
[25] M. Aydemir, A. Baysal, S. Özkar, L.T. Yıldırım, *trans*- and *cis*-Ru(II) aminophosphine complexes: syntheses, X-ray structures and catalytic activity in transfer hydrogenation of acetophenone derivatives, Inorg. Chim. Acta 367 (2011) 166–172.
[26] M. Aydemir, A. Baysal, S. Özkar, L.T. Yıldırım, Ruthenium complexes of aminophosphine ligands and their use as pre-catalysts in the transfer hydrogenation of aromatic ketones: X-ray crystal structure of thiophene-2-(*N*-diphenylthiophosphino)methylamine, Polyhedron 30 (2011) 796–804.
[27] M. Aydemir, A. Baysal, Cationic and neutral ruthenium(II) complexes containing both arene or Cp* and functionalized aminophosphines. Application to hydrogenation of aromatic ketones, J. Organomet. Chem. 695 (2010) 2506–2511.
[28] R.E. Morris, R.E. Aird, P. del Socorro Murdoch, H. Chen, J. Cummings, N.D. Hughes, S. Parsons, A. Parkin, G. Boyd, D.I. Jodrell, P.J. Sadler, Inhibition of cancer cell growth by ruthenium(II) arene complexes, J. Med. Chem. 44 (2001) 3616–3621.
[29] C. Aliende, M. Pérez-Manrique, F.A. Jalón, B.R. Manzano, A.M. Rodríguez, J.V. Cuevas, G. Espino, M.Á. Martínez, A. Massaguer, M. González-Bártulos, R. de Llorens, V. Moreno, Preparation of new half sandwich ruthenium arene complexes with aminophosphines as potential chemotherapeutics, J. Inorg. Biochem. 117 (2012) 171–188.
[30] R. Pettinari, C. Pettinari, F. Marchetti, B.W. Skelton, A.H. White, L. Bonfili, M. Cuccioloni, M. Mozzicafreddo, V. Cecarini, M. Angeletti, M. Nabissi, A.M. Eleuteri, Arene–ruthenium(II) acylpyrazolonato complexes: apoptosis-promoting effects on human cancer cells, J. Med. Chem. 57 (2014) 4532–4542.
[31] P. Tomšík, D. Muthná, M. Řezáčová, S. Mičuda, J. Ćmielová, M. Hroch, R. Endlicher, Z. Červinková, E. Rudolf, S. Hann, D. Stíbal, B. Therrien, G. Süss-Fink, [(p-MeC6H4Pri)2Ru2(SC6H4-p-but)3]cl (diruthenium-1), a dinuclear arene ruthenium compound with very high anticancer activity: an in vitro and in vivo study, J. Organomet. Chem. 782 (2015) 42–51.
[32] R. Pettinari, F. Marchetti, C. Pettinari, A. Petrini, R. Scopelliti, C.M. Clavel, P.J. Dyson, Synthesis, structure, and antiproliferative activity of ruthenium(II) arene complexes with N,O-chelating pyrazolone-based β-Ketoamine ligands, Inorg. Chem. 53 (2014) 13105–13111.
[33] A.K. Renfrew, A.D. Phillips, A.E. Egger, C.G. Hartinger, S.S. Bosquain, A.A. Nazarov, B.K. Keppler, L. Gonsalvi, M. Peruzzini, P.J. Dyson, Influence of structural variation on the anticancer activity of RAPTA-type complexes: ptn versus pta, Organometallics 28 (2009) 1165–1172.
[34] G. Von Poelhsitz, A.L. Bogado, M.P. de Araujo, H.S. Selistre-de-Araújo, J. Ellena, E.E. Castellano, A.A. Batista, Synthesis, characterization, X-ray structure and preliminary in vitro antitumor activity of the nitrosyl complex fac-[$RuCl_3$(NO)(dppf)], dppf = 1,1′-bis(diphenylphosphine)ferrocene, Polyhedron 26 (2007) 4707–4712.
[35] C.C. Golfeto, G.V. Poelhsitz, H.S. Selistre-de-Araújo, M.P.d. Araujo, J. Ellena, E.E. Castellano, L.G.L. Lopes, I.S. Moreira, A.A. Batista, Synthesis, characterization and cytotoxic activities of the [$RuCl_2$(NO)(dppp)(L)]PF_6 complexes, J. Inorg. Biochem. 104 (2010) 489–495.
[36] P. Appelt, F.D. Fagundes, G. Facchin, M. Gabriela Kramer, D.F. Back, M.A.A. Cunha, B. Sandrino, K. Wohnrath, M.P. de Araujo, Ruthenium (II) complexes containing 2-mercaptothiazolinates as ligands and evaluation of their antimicrobial activity, Inorg. Chim. Acta 436 (2015) 152–158.
[37] F. Fagundes, J. Reis, P. Appelt, D. Cavarzan, F. Murakami, R. Scopelliti, P. Dyson, M. de Araujo, p,t-[Ru(CO)(PR3)(tren)]2+ [R = Ph or p-tol; tren = tris(2-aminoethyl)amine], rare Ru(II) complexes bearing a simple tripodal tetradentate amine: Synthesis, characterization and antimicrobial activity, J. Coord. Chem. (2016), http://dx.doi.org/10.1080/00958972.2016.1211642.
[38] M.I.F. Barbosa, R.S. Corrêa, L.V. Pozzi, É.d.O. Lopes, F.R. Pavan, C.Q.F. Leite, J. Ellena, S.d.P. Machado, G.V. Poelhsitz, A.A. Batista, Ruthenium(II) complexes with hydroxypyridinecarboxylates: screening potential metallodrugs against *Mycobacterium tuberculosis*, Polyhedron 85 (2015) 376–382.
[39] F.B. do Nascimento, G. Von Poelhsitz, F.R. Pavan, D.N. Sato, C.Q.F. Leite, H.S. Selistre-de-Araújo, J. Ellena, E.E. Castellano, V.M. Deflon, A.A. Batista, Synthesis, characterization, X-ray structure and in vitro antimycobacterial and antitumoral activities of Ru(II) phosphine/diimine complexes containing the "SpymMe2" ligand, SpymMe2 = 4,6-dimethyl-2-mercaptopyrimidine, J. Inorg. Biochem. 102 (2008) 1783–1789.
[40] F.R. Pavan, G.V. Poelhsitz, M.I.F. Barbosa, S.R.A. Leite, A.A. Batista, J. Ellena, L.S. Sato, S.G. Franzblau, V. Moreno, D. Gambino, C.Q.F. Leite, Ruthenium(II) phosphine/diimine/picolinate complexes: Inorganic compounds as agents against tuberculosis, Eur. J. Med. Chem. 46 (2011) 5099–5107.
[41] WHO, Global tuberculosis report. (2016).
[42] B.A.V. Lima, R.S. Correa, A.E. Graminha, A. Kuznetsov, J. Ellena, F.R. Pavan, C.Q.F. Leite, A.A. Batista, Anti-*Mycobacterium tuberculosis* and cytotoxicity activities of ruthenium(II)/bipyridine/diphosphine/pyrimidine-2-thiolate complexes: the role of the non-coordinated N-atom, J. Braz. Chem. Soc. 27 (2016) 30–40.
[43] I.D. Aguiar, A. Tavares, A.C. Roveda Jr., A.C.H. da Silva, L.B. Marino, É.O. Lopes, F.R. Pavan, L.G.F. Lopes, D.W. Franco, Antitubercular activity of Ru (II) isoniazid complexes, Eur. J. Pharm. Sci. 70 (2015) 45–54.
[44] M.A.H. Bennett, T. N., T.W. Matheson, A.K. Smith, (η6-Hexamethylbenzene) ruthenium Complexes, (1982).
[45] N. Biricik, F. Durap, C. Kayan, B. Gümgüm, N. Gürbüz, İ. Özdemir, W.H. Ang, Z. Fei, R. Scopelliti, Synthesis of new aminophosphine complexes and their catalytic activities in C—C coupling reactions, J. Organomet. Chem. 693 (2008) 2693–2699.
[46] T. Mayer, H.-C. Boettcher, Structural characterization of *N*,*N*-bis(diphenylphosphanyl)propylamine, Z. Naturforsch., B: Chem. Sci. 67 (2012) 504–506.
[47] G.M. Sheldrick, SHELXS97. Program for Crystal Structure Solution, Univ. of Gottingen, Germany, 1997.
[48] G.M. Sheldrick, SHELXL97. Program for Crystal Structure Refinement, Univ. of Gottingen, Germany, 1997.
[49] J.-C. Palomino, A. Martin, M. Camacho, H. Guerra, J. Swings, F. Portaels, Resazurin microtiter assay plate: simple and inexpensive method for detection of drug resistance in *Mycobacterium tuberculosis*, Antimicrob. Agents Chemother. 46 (2002) 2720–2722.
[50] C. Daguenet, R. Scopelliti, P.J. Dyson, Mechanistic investigations on the hydrogenation of alkenes using ruthenium(II)-arene diphosphine complexes, Organometallics 23 (2004) 4849–4857.
[51] P. Tuberculosis, Drug screening, search for new drugs for treatment of tuberculosis, Antimicrob. Agents Chemother. 45 (2001) 1943–1946.
[52] E.A. Braude, F.C. Nachod, Determination of Organic Structures by Physical Methods, Academic Press, 1955.
[53] G. Anderegg, Pyridinderivate als Komplexbildner IX Die Stabilitätskonstanten von Komplexen mit (a) 2-aminomethyl-pyridin, (b) 6-methyl-2-aminomethyl-pyridin, (c) 2-pyridylhydrazin, (d) 2,2′-dipyridylamin und (e) 1-(α-pyridylmethylen)-2-(α′-pyridyl)-hydrazin, Helv. Chim. Acta 54 (1971) 509–512.
[54] H.K. Hall, Correlation of the base strengths of amines1, J. Am. Chem. Soc. 79 (1957) 5441–5444.